

## Collective Motion in a System of Motile Elements

Naohiko Shimoyama, Ken Sugawara, Tsuyoshi Mizuguchi, Yoshinori Hayakawa, and Masaki Sano

*Research Institute of Electrical Communication, Sendai, 980-77, Japan*

(Received 28 August 1995)

Clusters of biological organisms often show diverse collective motions. Considering the physical properties of active elements with mutual interactions, we propose a mathematical model of collective motion. Several kinds of cluster motion seen in nature, including collective rotation, chaos, and wandering, occur in computer simulations of our deterministic model. By introducing a set of dimensionless parameters, we categorize the collective motions and obtain their phase diagram. We analyze the collective motions with a disorder parameter and Lyapunov spectra to characterize their transitions. [S0031-9007(96)00218-9]

PACS numbers: 87.10.+e, 05.45.+b, 87.45.-k

Many biological organisms form groups which we consider as cooperative systems of self-driven or motile elements. In biological systems, the collective motion of motile elements show extreme diversity of dynamics and patterns [1–4]. For example, migrant fish, such as the sardine, tend to school by aligning their heading and keeping mutual distance. In flocks birds, cranes, geese, and pelicans migrate in well-ordered formations with constant cluster velocity. Passerines fly in wandering, disordered aggregates. Insects, such as the mosquito, fly at random within spatially limited swarms. Cooperative motion in a bacterial colony is other example which is attracting wide interests both from theoretical and experimental sides [5–8]. The benefit of such collective motion has been discussed [9,10]. However, the variety of dynamics and patterns which depend on the time and length scales has not been considered from a general point of view. The time and length scales, i.e., size, mass, and speed, differ tremendously from, e.g., bacteria to birds; the characteristics of the active elements may depend on such parameters.

How can we incorporate diverse collective animal behavior in a common framework? In this Letter, we propose deterministic kinetic equations of motions for interacting elements which describe various collective behaviors. We characterize the different types of collective behavior and obtain their phase diagram. By introducing proper nondimensional parameters, we show that a few physical quantities can categorize every state. Our model has well-ordered regular and chaotic motion which we examine with a disorder parameter and Lyapunov spectra. The transition between them does not require random fluctuations.

Many model equations claim to explain the collective motion of animals [11]. Most postulate that individuals are simply particles with the mutual interactions and motive force. The resulting collective motion is mostly regular and ordered. Swarming, disordered aggregates, and wandering require external random perturbations. To generalize these models, we introduce the *heading unit vector*  $\vec{n}_i$ . Large birds often glide. In a glide, the heading,  $\vec{n}_i$ , and

the velocity vector,  $\vec{v}_i$ , need not be parallel. Therefore we assume that  $\vec{n}_i$  and  $\vec{v}_i$  relax to parallel with relaxation time  $\tau$ . The state variables for the  $i$ th element are the position vector  $\vec{r}_i$ , the velocity vector  $\vec{v}_i$ , and the heading unit vector  $\vec{n}_i$  (see Fig. 1), and obey the following dynamics:

$$m \frac{d\vec{v}_i}{dt} = -\gamma\vec{v}_i + a\vec{n}_i + \sum_{j \neq i} \alpha_{ij} \vec{f}_{ij} + \vec{g}_i, \quad (1)$$

$$\tau \dot{\vec{n}}_i/dt = \vec{n}_i \times \vec{v}_i/|\vec{v}_i| \times \vec{n}_i \quad (i = 1, 2, \dots, N). \quad (2)$$

Equation (1) is Newton's equation of motion for particles of mass  $m$ ;  $\gamma$  is the resistive coefficient based on Stokes's law. The locomotive force  $a$  acts in the heading direction  $\vec{n}_i$ . The term,  $\vec{f}_{ij}$ , represents short range attractive and repulsive forces between the  $i$ th and  $j$ th elements, and  $\vec{g}_i$  is the force toward the gravitational center of the group. For simplicity, we limit ourselves to motions in two dimensions in this study, but the model is easily extensible to three dimensions.

As reported by Breder [12] based on the observations for fish schooling, within a certain range of space, interactive force between animals might be represented with

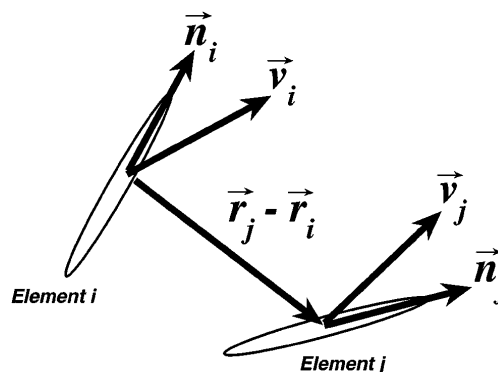


FIG. 1. Schematic diagram of the model with two elements.  $\vec{n}$  is the heading unit vector,  $\vec{r}$  the position vector, and  $\vec{v}$  the velocity vector.

intermolecularlike attraction and repulsion. Here we assume that the interaction force is given by

$$\vec{f}_{ij} = -c_\ell \left[ \left( \frac{|\vec{r}_j - \vec{r}_i|}{r_c} \right)^{-3} - \left( \frac{|\vec{r}_j - \vec{r}_i|}{r_c} \right)^{-2} \right] \times \left( \frac{\vec{r}_j - \vec{r}_i}{r_c} \right) \exp(-r/r_c), \quad (3)$$

where  $r_c$  is the optimal distance between neighbors as well as the range of the force. The interaction need not be isotropic. The interaction with elements in front of a given element is stronger than with those behind. Therefore, we introduce a direction sensitivity factor described by

$$\alpha_{ij} = 1 + d[\vec{n}_i \cdot (\vec{r}_j - \vec{r}_i)/|\vec{r}_j - \vec{r}_i|] \quad (0 \leq d \leq 1), \quad (4)$$

and multiply it by  $\vec{f}_{ij}$  in the interaction term. When  $d = 0$ , the interaction is isotropic. Furthermore, we introduce globally attraction force  $\vec{g}_i$  given by

$$\vec{g}_i = c_g(\vec{g} - \vec{r}_i)/N|\vec{g} - \vec{r}_i|, \quad (5)$$

where  $\vec{g}$  is the center of the group, i.e.,  $\vec{g} = \sum_i \vec{r}_i/N$ . In the following discussions, we assume these two interaction forces have the same degree of magnitude, i.e.,  $c = c_\ell = c_g$ , if not specified.

To investigate the qualitative properties of our model, we carried out numerical simulations for various control parameters and observed the collective motions. Here we concentrate on the viscous regime in which the left-hand side of Eq. (1) is negligible, because of its variety of behavior. Because of the long range attractive force  $\vec{g}_i$ , elements gather into a single cluster, regardless of initial location, as long as the locomotive force  $a$  is not too large. When  $N$  is of order ten, as in most natural groupings, we found several distinct collective behaviors. Corresponding conformations of elements and the trajectory of the center of the cluster are illustrated in Fig. 2.

(1) *Marching*: When the anisotropy of mutual attraction is small, the elements form a regular triangular crystal moving at constant velocity. We call this motion a marching state.

(2) *Oscillation (circling)*: Several group motions exhibit regular oscillations, including (i) wavy motion of the cluster along a linear trajectory, (ii) a cluster circling a center outside the cluster, (iii) a cluster circling a center inside the cluster. Oscillatory clusters often occur near the boundary between wandering, and the oscillation and marching may coexist for some parameters.

(3) *Wandering*: For nonzero  $d$ , the center of the cluster can wander quite irregularly, while the latticelike order inside the cluster persists. The mutual position of elements rearranges intermittently according to chaotic changes in the direction of motion.

(4) *Swarming*: Beyond the wandering regime, we found more irregular motion, where the regularity within the cluster fails, although the cluster persists. This is a behavior reminiscent of a cloud of mosquitoes.

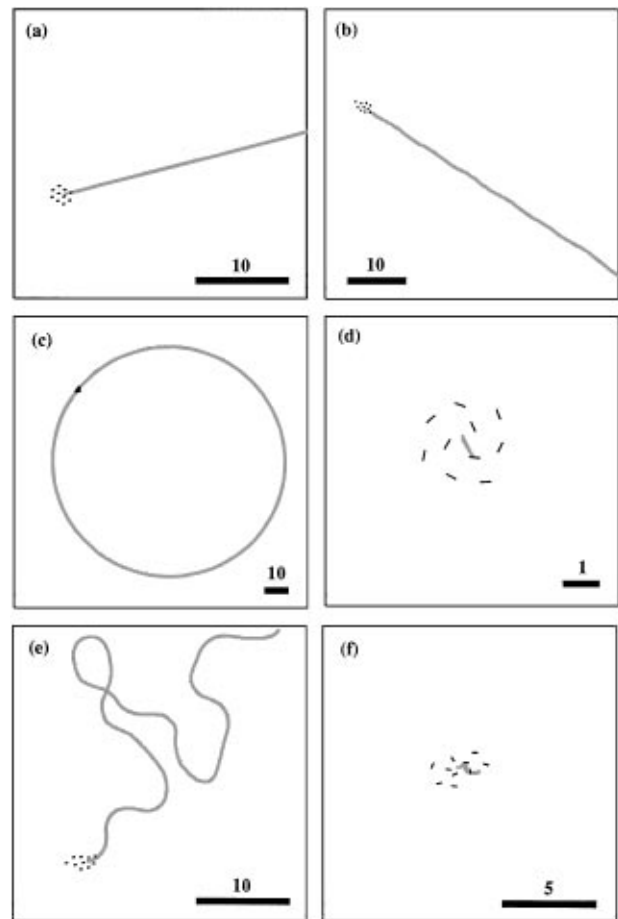


FIG. 2. Patterns of clusters and the trajectories of their centers of mass in viscous regime: (a) marching, (b) oscillatory (wavy), (c) oscillatory (circling), (d) oscillatory (spiral), (e) wandering, and (f) swarming. Solid bars represent motive elements, and gray line is the trajectory of the center of the cluster.

In an inertial regime, i.e., when  $m/\gamma$  is large, the regular structure within a cluster is less stable than in the viscous regime. For small enough  $d$ , regular marching occurs, but it takes a long time to achieve steady motion. We also found irregular clustering in which each element has longer free distances than  $r_c$ .

Marching and oscillation form an ordered phase, while the others form a disordered phase. We refer to the transition between order and disorder as the marching-swarming transition. To characterize the different collective motions quantitatively, we introduce a disorder parameter. Letting the velocity of the cluster at a moment  $t$  be

$$\vec{V}(t) = \frac{1}{N} \sum_i \vec{v}_i(t). \quad (6)$$

The fluctuation in velocity space can be evaluated by averaging the rms velocity deviation over time:

$$\langle (\Delta v)^2 \rangle \equiv \left\langle \frac{1}{N} \sum_i |\vec{v}_i(t) - \vec{V}(t)|^2 \right\rangle. \quad (7)$$

This quantity gives zero in ordered motions and nonzero in disordered motions. Using the parameter, the order disorder transition appears as a change in disorder parameter.

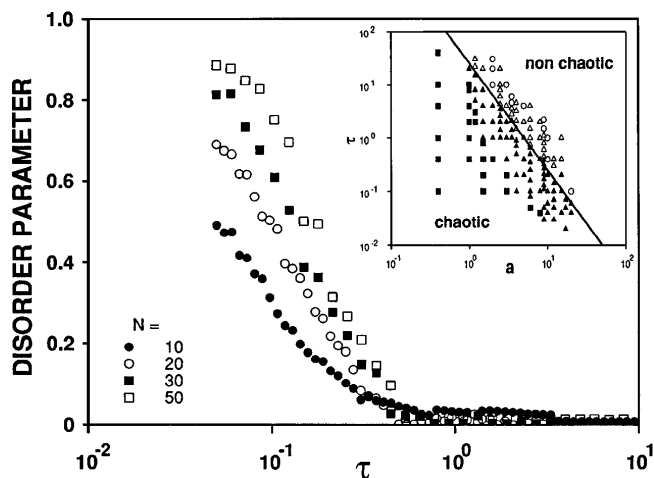


FIG. 3. Characterization of the marching-swarming transition in the viscous regime using disorder parameter  $\langle(\Delta v)^2\rangle^{1/2}/\langle V^2\rangle^{1/2}$  for various particle number  $N$ . The inset is a phase diagram in  $a$ - $\tau$  space showing chaotic (black marks) and nonchaotic (white marks) states.  $c = 5$ ,  $m = 1$ ,  $\gamma = 10$ ,  $a = 5$ , and  $d = 1$  are used to obtain main figure.

In Fig. 3, the disorder parameter is plotted by changing  $\tau$  for several numbers of elements up to fifty. As increasing the number of elements, the transition can be seen clearer. Swarming state corresponds to the motion with a larger  $\langle(\Delta v)^2\rangle^{1/2}/\langle V^2\rangle^{1/2}$  value, and wandering and swarming states are continuous.

We obtained several phase diagrams for the marching-swarming transition in  $a$ - $\tau$ ,  $\gamma$ - $\tau$ ,  $c$ - $\tau$ , and  $r_c$ - $\tau$  spaces, respectively. Here we chose parameters in the viscous regime where the inertial term in Eq. (1) is negligible. The inset of Fig. 3 shows an example of phase diagrams for varying  $a$  and  $\tau$ . At the transition line, we obtained  $a^* \sim \tau^{*-1/2}$ ,  $\gamma^* \sim \tau^*$ ,  $c^* \sim \tau^*$ , and  $r_c^* \sim \tau^*$ , where \* signifies the boundary between the states. These transition lines can be represented in a simple form by introducing dimensionless parameters. Introducing the nondimensional variables  $v'$ ,  $t'$ ,  $r'$  defined by  $v = V_0 v'$ ,  $t = T_0 t'$ , and  $r = L_0 r'$ , where  $L_0 \equiv r_c$ ,  $V_0 \equiv a/\gamma$ , and  $T_0 \equiv L_0/V_0$ , we obtain the following nondimensional equations of motion for the  $i$ th element:

$$R \frac{d\vec{v}'_i}{dt'} = -\vec{v}'_i + \vec{n}_i + \frac{1}{Q} \left( \sum_{j \neq i} \alpha_{ij} \vec{f}_{ij} + \vec{g}_i \right), \quad (8)$$

$$\frac{1}{P} \frac{dn_i}{dt'} = \vec{n}_i \times \frac{\vec{v}'_i}{|\vec{v}'_i|} \times \vec{n}_i. \quad (9)$$

We have three independent dimensionless parameters  $P$ ,  $Q$ , and  $R$  defined by

$$P \equiv r_c \gamma / a \tau, \quad (10)$$

$$Q \equiv a / c, \quad (11)$$

$$R \equiv m a / \gamma^2 r_c. \quad (12)$$

The physical interpretation of each parameter is  $P$  is the ratio of the typical time scale for heading relaxation,  $\tau$

and the “mean free time,”  $r_c \gamma / a$ .  $Q$  is the ratio of the magnitude of the motive force and the interaction force with neighbors.  $R$  is the ratio of the inertial force and the viscous force, which resembles a “Reynolds number” in fluid mechanics.  $R \ll 1$  corresponds to the viscous regime.  $d$  and  $N$  are additional dimensionless parameters.

Using the dimensionless parameters  $P$  and  $Q$ , the proportionalities between parameters on transition lines simplify to  $G^* \equiv P^*/Q^* = \text{const}$  as shown in Fig. 4. Since  $R \ll 1$ ,  $G$  is independent of  $R$ , but may be a function of  $d$  for fixed  $N$ . Our numerical results in Fig. 3, however, indicate that  $G^*$  is insensitive to  $N$ . Therefore we conjecture that the marching-swarming transition occurs for

$$G = G^*(d), \quad (13)$$

for  $R \ll 1$ . We confirmed that in the  $G$  vs  $d$  plane different sets of experiments collapsed in the same transition line. Asymptotic behavior for  $N \rightarrow \infty$  has to be studied by more systematic numerical calculations.

The Lyapunov spectrum helps to characterize collective and chaotic behaviors with many degrees of freedom [13,16]. Each of our elements has 5 degrees of freedom  $(x, y, v_x, v_y, \theta)$ ; thus the  $N$  cluster has  $5N$  variables. Each element has three neutral modes associated with symmetries; two correspond to spatial translation invariance  $(x, y) \rightarrow (x + x_0, y + y_0)$ , and one corresponds to rotation invariance  $\theta \rightarrow \theta + \theta_0$ . In marching, the center of mass of the cluster behaves like a single element. In fact, three out of the  $5N$  modes become neutral modes. The other  $5N - 3$  modes have negative Lyapunov exponents, representing the stability of the marching cluster against disturbances. We show Lyapunov spectra for different states in Fig. 5. The Lyapunov spectrum characterizes marching, wandering and swarming as follows.

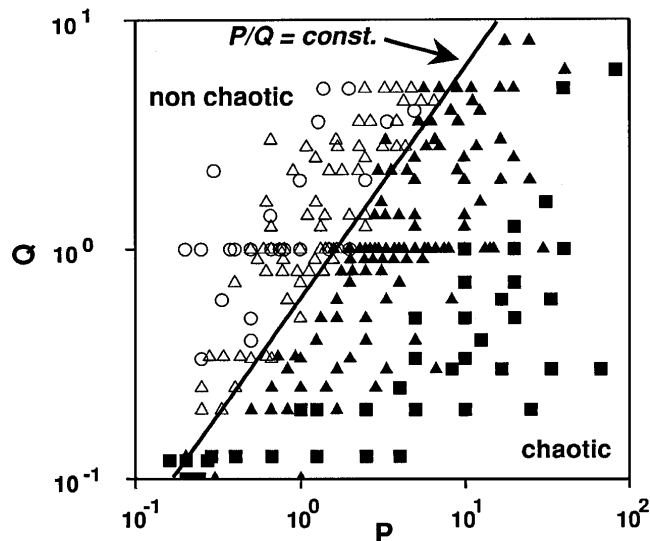


FIG. 4. Phase diagram of collective motions for varying nondimensional parameters  $P$  and  $Q$  in the viscous regime ( $R < 0.05$ ). In the diagram, white circles indicate marching, white triangles oscillation, black triangles wandering, and black rectangles swarming.

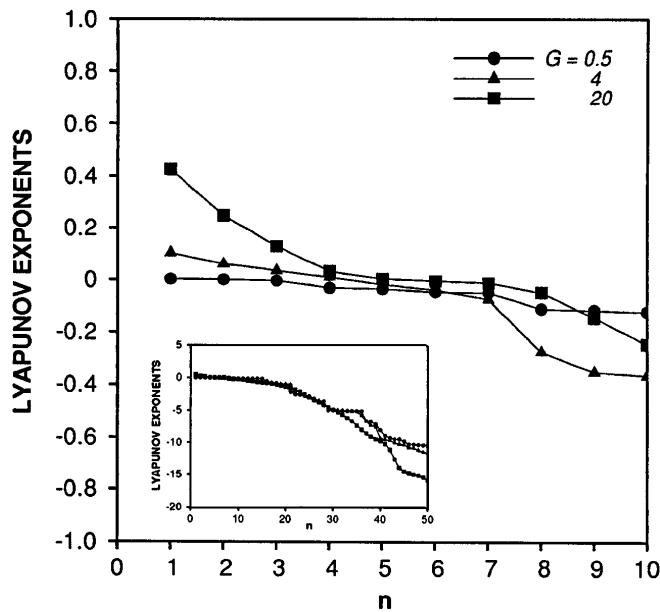


FIG. 5. Typical Lyapunov spectrum for marching ( $G = 0.5$ ,  $d = 1$ ) (circles), wandering ( $G = 4$ ,  $d = 1$ ) (triangles), and swarming ( $G = 20$ ,  $d = 1$ ) (rectangles). The Lyapunov exponents  $\lambda_n$  are plotted in descending order of magnitude with numbering  $n$ . Other parameters are chosen as  $N = 10$ ,  $\gamma = 10$ ,  $c = 5$ ,  $r_c = 1$ , and  $m = 1$ .

(1) *Marching or oscillating (circling)*: No positive exponents, but three or four neutral modes, respectively, for straight marching or wavy marching. The spectrum has a plateau of negative exponents. The number of modes in the plateau increases with  $N$ .

(2) *Wandering*: More than one positive exponent appears, followed by three neutral modes. The plateau in the negative exponents disappears and the spectrum is smooth.

(3) *Swarming*: The number of positive exponents is of order  $N$  and increases as the spontaneous chaotic fluctuations of individuals increases in the swarm.

To compare the simulation to observations of real animals, we rewrite  $G$  as follows:

$$G = cr_c\gamma/a^2\tau = (c/a)(L/V\tau). \quad (14)$$

The *optimal mutual distance*,  $r_c$ , is of the same order as the body length  $L$  [4,14], so we set  $r_c \sim L$ . For the characteristic time scale,  $\tau$ , we use the fluttering period of the wings for birds or insects.  $Q = a/c$  is the ratio between the locomotive force and the interaction force, and we assume  $Q \sim 1$  for simplicity. We compare three cases: crane, sparrow, and mosquito. The body length  $L$ , flutter-

ing period  $\tau$ , and velocity  $V$  are as follows [15]. Crane:  $M \sim 10^4$  g,  $\tau \sim 1$  sec,  $L \sim 10^2$  cm,  $V \sim 10^3$  cm/sec. Sparrow:  $M \sim 10^2$  g,  $\tau \sim 0.1$  sec,  $L \sim 10$  cm,  $V \sim 10^2$  cm/sec. Mosquito:  $M \sim 10^{-3}$  g,  $\tau \sim 10^{-3}$  sec,  $L \sim 10^{-1}$  cm,  $V \sim 1$  cm/sec. The nondimensional parameter  $G$  for each animal is  $G_{\text{crane}} \sim 0.1$ ,  $G_{\text{sparrow}} \sim 1$ , and  $G_{\text{mosq}} \sim 10^2$ . As shown above, the transition from marching to wandering occurs around  $G \sim 1$  independent of the number of elements, agreeing with the observation that mosquitoes swarm while flocks of crane form ordered formations. Furthermore, the flock of sparrows shows wandering consistent with the value of  $G$  close to the transition point. The estimate may fail when  $R$  (the Reynolds number) is large, though the eddy viscosity may possibly result in a lower effective Reynolds number.

We are grateful to James A. Glazier for a careful reading of the manuscript and illuminating comments. Part of this work is supported by the Japanese Grant-in-Aid for Science Research Fund from the Ministry of Education, Science and Culture (Grant No. 07243201).

- [1] E. O. Wilson, *Sociobiology* (Harvard, Cambridge, MA, 1975).
- [2] L. Edelstein-Keshet, in *Lecture Notes in Biomathematics*, edited by W. Alt and G. Hoffmann (Springer, Berlin, 1990), Vol. 89, p. 528, and references therein.
- [3] B. L. Partridge, *Sci. Am.* **246**, No. 6, 90 (1982).
- [4] M. Inoue, *Schooling of Fishes; behavior* (Kaiyo-shuppan, Tokyo, 1981) (in Japanese).
- [5] T. Vicsek, A. Czirok, E. Ben-Jacob, I. Cohen, and O. Shochet, *Phys. Rev. Lett.* **75**, 1226 (1995).
- [6] A. Czirok, E. Ben-Jacob, I. Cohen, and O. Shochet, 1995 (to be published).
- [7] E. O. Budrene and H. C. Berg, *Nature (London)* **349**, 630 (1991).
- [8] T. Matsuyama, R. M. Harshey, and M. Matsushita, *Fractals* **1**, 302 (1993).
- [9] D. H. Cushing, *Nature (London)* **218**, 918 (1968).
- [10] D. Weihs, *Nature (London)* **245**, 48 (1973).
- [11] H. Niwa, *J. Theor. Biol.* **171**, 123 (1994).
- [12] C. M. Breder, *Ecology* **35**, 361 (1954); *Fish. Bull.* **74**, 471 (1976).
- [13] J. P. Eckmann and D. Ruelle, *Rev. Mod. Phys.* **57**, 617 (1985).
- [14] E. Shaw, *FAO Fish Rep.* **62**, 217 (1969).
- [15] A. Azuma, *The Biokinetics of Flying and Swimming* (Springer-Verlag, Tokyo, 1992).
- [16] I. Shimada and T. Nagashima, *Prog. Theor. Phys.* **61**, 1605 (1979).